Computer Networks 53 (2009) 883–895

Contents lists available at ScienceDirect

Computer Networks

journal homepage: www.elsevier.com/locate/comnet

Channel access using opportunistic reservations and virtual MIMO ☆

Xin Wang [a,*], J.J. Garcia-Luna-Aceves [a,b], Hamid R. Sadjadpour [c]

[a] Department of Computer Engineering, University of California, Santa Cruz, 1156 High Street, Santa Cruz, CA 95064, United States
[b] Palo Alto Research Center (PARC), 3333 Coyote Hill Road, Palo Alto, CA 94304, United States
[c] Department of Electrical Engineering, University of California, Santa Cruz, 1156 High Street, Santa Cruz, CA 95064, United States

ARTICLE INFO

Article history:
Received 23 October 2007
Received in revised form 21 July 2008
Accepted 8 October 2008
Available online 1 November 2008

Responsible Editor: L. Lenzini

Keywords:
Channel access
Reservation
Virtual MIMO

ABSTRACT

We propose ORCHESTRA, a channel-access protocol that uses reservations and virtual MIMO to provide high throughput and bounded channel-access delays. The channel-access process is divided into a contention-based access period and a scheduled access period. To attain high throughput, nodes build a channel schedule using the contention-based access period, and utilize the spatial multiplexing gain of virtual MIMO links in the scheduled access period. To attain bounded channel-access delays, nodes reserve time slots through opportunistic reservations. We evaluate the performance of ORCHESTRA through numerical analysis and simulations, and show that it results in much better throughput, delay, and jitter characteristics that simply using MIMO nodes together with scheduled access (i.e., NAMA) or contention-based access (i.e., IEEE 802.11 DCF).

1. Introduction

Recent advances in ad hoc networks have stimulated the support of voice-related applications such as voice over wireless IP. These applications need to coexist with data-centric applications. To better support such integrated voice and data traffic in an ad hoc network, the underlying channel-access protocol needs to satisfy two requirements: high channel utilization and bounded channel-access delay.

Multiple-input multiple-output (MIMO) techniques can increase channel capacity significantly through the use of multiple antennas. In a point-to-point MIMO channel, the multiple antenna arrays increase the spatial degrees of freedom (DOF) and can provide spatial multiplexing gain or spatial diversity gain [1]. Consider a system with N transmit and M receive antennas, in order to achieve the spatial multiplexing gain, the incoming data are demultiplexed into N distinct streams and each stream is transmitted from a different antenna with equal power at the same frequency. Foschini et al. [2] has shown that the multiplexing gain can provide a linear increase in the asymptotic link capacity as long as both transmit and receive antennas increase. In rich multipath environments, the transmitted data streams fade independently at the receiver and the probability that all data streams experience a poor channel at the same time is reduced. This contributes to the spatial diversity gain of the MIMO channel. In order to achieve spatial diversity gain, each stream is transmitted using different beamforming weights to achieve a threshold gain at the specified receiver while at the same time nulling coexisting, potentially interfering transmitter–receiver pairs. The spatial diversity gain can be used to reduce the bit error rate (BER) or increase the transmission range of the wireless links [3]. We denote by H_{ij} the channel coefficient

☆ This work was partially sponsored by the US Army Research Office under Grants W911NF-04-1-0224 and W911NF-05-1-0246, by the National Science Foundation under Grant CNS-0435522, by DARPA through Air Force Research Laboratory (AFRL) Contract FA8750-07-C-0169, and by the Baskin Chair of Computer Engineering. The views and conclusions contained in this document are those of the authors and should not be interpreted as representing the official policies, either expressed or implied, of the Defense Advanced Research Projects Agency or the US Government.

* Corresponding author. Tel.: +1 831 4595436; fax: +1 831 4594829.
E-mail addresses: wangxin@soe.ucsc.edu (X. Wang), jj@soe.ucsc.edu (J.J. Garcia-Luna-Aceves), hamid@soe.ucsc.edu (H.R. Sadjadpour).

1389-1286/$ - see front matter © 2008 Elsevier B.V. All rights reserved.
doi:10.1016/j.comnet.2008.10.010

matrix between sender i and receiver j. H_{ij} can be estimated by the receiver through pilot symbols, but it is unknown at the sender.

Spatial multiplexing and spatial diversity gains cannot be maximized at the same time, and so there is a tradeoff between how much of each type of gain any scheme can extract [1]. In this paper, we use virtual antenna arrays to emulate a MIMO system, which can provide the same type of antenna gains and have a higher channel capacity. We propose ORCHESTRA, a channel-access protocol that uses reservations and virtual MIMO to provide high throughput and bounded channel-access delays. The channel-access process is divided into a contention-based access period and a scheduled access period. To attain high throughput, nodes build a channel schedule using the contention-based access period, and utilize the spatial multiplexing gain of virtual MIMO links in the scheduled access period. To attain bounded channel-access delays, nodes reserve time slots through opportunistic reservations. Section 2 provides a summary of related work, and Section 3 describes ORCHESTRA. Section 4 analyzes the frame length, throughput, worst-case channel-access delay, and convergence time of ORCHESTRA. Section 5 evaluates the performance of ORCHESTRA under multi-hop scenarios through simulations, and compares it with alternative designs based on the application of MIMO nodes to IEEE 802.11 DCF and a basic schedule-based channel-access protocol.

2. Related work

Sundaresan et al. [4] proposed a fair stream-controlled medium access protocol for ad hoc networks with MIMO links. This work assumes that the receiver can successfully decode all the spatially multiplexed streams when the total number of incoming streams is smaller than or equal to its DOFs. A graph-coloring algorithm is used to find the receivers that may be overloaded with more streams than they can receive, and then fair link allocation and stream control are applied to leverage the advantage of spatial multiplexing.

SD-MAC [5], NULLHOC [6], and SPACE-MAC [7] all take advantage of spatial diversity. SD-MAC uses the spatial degrees of freedom embedded in the MIMO channels to improve the link quality and multi-rate transmissions. It uses the preamble symbols of each packet to convey the channel gains. RTS and CTS are transmitted using a default rate, while data packets are transmitted using multi-rate transmissions. NULLHOC divides the channel into a control channel and a data channel. It uses RTS/CTS handshake in the control channel to keep track of the active transmitters and receivers in the neighborhood and distributes the required transmit and receive beamforming weights. After a receiver obtains an RTS from the transmitter, it calculates its weight vector to null interfering transmissions and conveys the weights to the transmitter using a CTS. The transmitter then calculates its weights to null active receivers in the neighborhood and to obtain unity gain to the desired receiver. Lastly, the receiver and the transmitter convey their selections of weight vectors to all their respective inactive and receiving neighbors. Compared with NULLHOC, SPACE-MAC uses a single channel for the transmission of control and data packets. A node estimates the channel coefficient after it receives the RTS/CTS packets. When a node other than the designated receiver obtains an RTS, it estimates the effective channel matrix and adjusts the weight vector such that the signal from the sender of the RTS is nullified for the duration of time specified in the RTS duration field. When a node other than the sender of the RTS receives the CTS, it estimates the effective channel and stores the weight vector for the duration specified in the CTS duration field.

The virtual antenna array (VAA) approach was first introduced by Dohler [8]. A base-station array consisting of several antenna elements transmits a space–time encoded data stream to the associated mobile terminals which can form several independent VAA groups. Each mobile terminal within a group receives the entire data stream, extracts its own information and concurrently relays further information to the other mobile terminals. It then receives more of its own information from the surrounding mobile terminals and, finally, processes the entire data stream. VAA offers theoretically much more in terms of capacity bounds and data throughput.

Jakllari et al. [9] proposed a multi-layer approach for ad hoc networks using virtual antenna arrays. By using the spatial diversity gain and cooperative transmission among different nodes, their approach forms a virtual MIMO link that increases the transmission range and reduces the route path length. However, this approach requires the virtual MIMO links to be bi-directional. In addition, when there are not enough collaborating nodes around the receiver, the sender cannot cooperate with other nodes to utilize the spatial diversity gain.

3. Orchestra

3.1. Motivation

The ergodic (mean) capacity for a complex additive white Gaussian noise (AWGN) MIMO channel can be expressed by [10,11]:

$$C = E_H\left\{\log_2\left[\det\left(I_M + \frac{P_T}{\sigma^2 N_T} HH^{\dagger}\right)\right]\right\}, \quad (1)$$

where P_T is the transmit power constraint, N_T is the number of transmit antennas, M is the number of receive antennas, H is the channel matrix, σ^2 is the variance of AWGN and superscript $\dagger$ denotes the complex conjugate transpose. E_H denotes the expectation over all channel realizations.

The above expression for C demonstrates that, under the constraint of constant total transmit power per node, increasing the number of receive antennas increases the system capacity. However, with the increase of the transmit antennas, the system capacity becomes a constant if the number of receive antennas is fixed. Based on this observation, we consider the specific virtual MIMO system shown in Fig. 1. Each node can transmit using only one antenna, but can decode multiple simultaneous transmissions using up to M antennas.

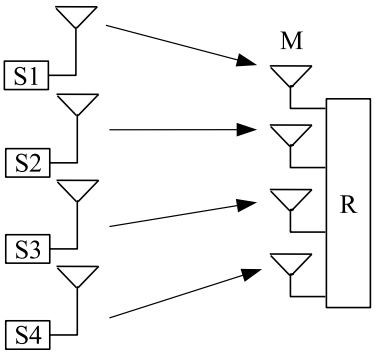

Fig. 1. Virtual MIMO system.

The spatial multiplexing gain of the virtual MIMO link cannot be applied directly to the MAC protocol. When the number of simultaneous transmissions is more than the number of receive antennas, the performance of the decoder decreases and the computational complexity of the receiver increases significantly. In order to correctly achieve the spatial multiplexing gain, senders need to form a schedule to coordinate the simultaneous transmissions. However, it is impossible to use perfect channel scheduling in a multi-hop ad hoc network, and random channel access has to be used to some extent. Accordingly, ORCHESTRA is built around a hybrid channel-access approach based on opportunistic reservations to leverage the capabilities provided by virtual MIMO links.

3.2. Scheme overview

The major problems that distributed channel-access protocols for ad hoc networks need to solve are:

- Allocating fairly the bandwidth across different transmitter–receiver pairs.
- Handle the control packets.
- Handle conflicts of the scheduling results across multiple hops.

In order to solve the above problems, we propose the following scheduling rule in ORCHESTRA. Receiver-based fair transmission scheduling is used to allocate bandwidth among different transmitters. The exponential back-off is used to reduce control packets collisions from different transmitters, while spatial diversity gain is used to reduce the control packets collisions from different receivers. Scheduling conflicts are resolved according to the topology information maintained by nodes.

ORCHESTRA divides the channel-access procedure into two parts: contention-based access and schedule-based access. When nodes start from scratch, nodes first send request-to-send (RTS) packets through the contention-based access, which include the topology, channel state and traffic flow information. Receivers form a fair transmission scheduling according to the past bandwidth share of different links and send the schedule results through clear-to-send (CTS) packets. CTS packets are transmitted through the utilization of spatial diversity gain to reduce collisions.

During subsequent time frames, in order to provide the bounded channel-access delay, nodes reserve the time slots in the schedule-based access through sending ready-to-receive (RTR) packets at the beginning of the contention-based access period, then only the sub-set of idle nodes whose destination is the node indicated in the RTR packet could send request-to-send (RTS) packets. When RTR or RTS transmissions experience collisions, nodes back-off across time slots and retransmit.

After the transmission schedule is formed, data packets are transmitted through schedule-based access taking advantage of spatial multiplexing gain.

The scheduling goal of ORCHESTRA is first to form the fair one-hop transmission scheduling, then resolve the scheduling conflicts over multiple hops by comparing the corresponding achieved spatial multiplexing gains.

3.3. Channel organization

A time frame (T_f) is made up of L time slots. We assume the channel status does not change within a time slot (T_s), which equals to approximately 1 ms. Each node is synchronized on slot systems and nodes access the channel based on slotted time boundaries. Each time slot is numbered relative to a consensus starting point. A time slot is made up of the contention-based access period and the schedule-based access period, as shown in Fig. 2.

3.4. Contention-based access period

During the contention-based access period, nodes exchange the neighbor information and form a transmission schedule. It is further divided into a ready-to-receive (RTR) section, a request-to-send (RTS) section and a clear-to-send (CTS) section.

3.5. RTR section

A node that determines itself to be the intended receiver of other nodes or observes a broadcast transmission request identifies itself as a *receiver*. The RTR section is used by a receiver j to send an RTR packet that indicates: (a) The current slot t is occupied by j and only the nodes that have packets targeted to j can transmit in slot t; (b) the list of senders that have successfully reserved transmissions in slot t for receiver j; and (c) the number of senders targeted for receiver j (K_s^j). This information helps each sender to decide how many slots it should reserve in a time frame. We denote the overall number of transmission pairs in

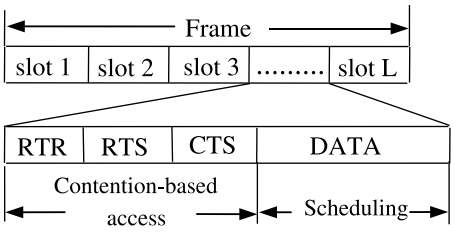

Fig. 2. Frame and time slot structure.

the two-hop range as K_s, $K_s = \sum_j K_s^j$, then each sender should reserve at least $\left\lfloor \frac{L}{K_s} \right\rfloor$ slots in a frame.

Based on the neighbor information collected, each receiver chooses the time slots it occupies in the next frame and sends an RTR packet in the RTR section of those slots. The length of the RTR section is T_{RTR}, where T_{RTR} is the transmission time for an RTR packet.

3.6. RTS section

The RTS section is used to exchange neighbor information and channel-state information. RTS section is made up of multiple mini-slots, as shown in Fig. 3.

The length of the RTS section is $L_{RTS} = M \times T_{PS} + R \times (T_{RTS} + T_{PS})$, where T_{PS} is the transmission time for pilot symbols, T_{RTS} is the transmission time for an RTS packet.

If a sender i observes an RTR packet indicating that m ($m \leqslant M$) senders (including i) have successfully reserved transmissions, it sends the pilot symbols in the first M mini-slots of the RTS period, according to the sequence indicated in the RTR packet. The pilot symbols are needed by the receiver to estimate the channel status and utilize the spatial multiplexing gain. Otherwise, it randomly picks one of the remaining R mini-slots and send an RTS packet along with the pilot symbols.

The RTS packet includes the following items:

- The intended receiver j.
- The past bandwidth share of link (i,j) (B_{ij}). B_{ij} is defined as the percentage of successful transmissions of link (i,j) over the past five time frames.
- Antenna weight W_i which will be used by sender i to receive the CTS packet. W_i is initialized randomly by the sender i.
- Its one-hop neighbor list and whether a one-hop neighbor is a receiver (if a node did not receive any packets from a neighbor during the past 2 time frames, it will remove the neighbor from the one-hop neighbor list).

After receiving the pilot symbols from sender i, receiver j uses the pilot symbols to estimate the channel matrix between i and j ($H_{i,j}$).

3.7. CTS section

The CTS section is used to form the transmission scheduling and broadcast the scheduling results through the transmissions of CTS packets. It includes three steps.

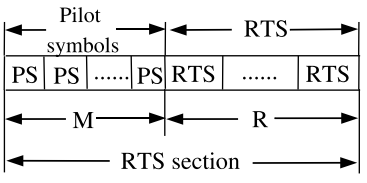

Fig. 3. RTS section.

3.7.1. Receiver-based channel scheduling formation

Each receiver forms a channel schedule $S(t)$ based on the information collected in the RTS section. The data slot number of the schedule-based transmission period is t; $t \in 1,\ldots,N_{data}$; and N_{data} is the length of schedule-based transmission period, which is discussed in Section 3.9. We assume that two distinct links $i = (s_i, r_i)$ and $j = (s_j, r_j)$, (where r_i and r_j are receivers), *interfere* with each other if one of the transmitters $s_i(s_j)$ is in the transmission range of the other link's receiver $r_j(r_i)$. The indicator function $I(i,j)$ equals 1 if link i,j interfere with each other; otherwise, it equals zero. With this, we formulate the transmission scheduling problem as follows:

$$\begin{aligned} \max \quad & \sum_{t=1}^{N_{data}} \sum_{i=1}^{|S(t)|} \log B_i \\ \text{s.t.} \quad & I(i,j) = 0 \quad \forall i,j \in S(t), \ \ i \neq j, \\ & |S(t)| \leqslant M \quad \forall t \in 1,\ldots,N_{data}, \end{aligned} \tag{2}$$

where B_i is the past bandwidth share of link i, it is obtained through the exchange of the RTS packets, as indicated in Section 3.6.

The objective of the optimization is to achieve the proportional fairness among different links. The first constraint ensures the scheduling is collision-free. The second constraint guarantees that the number of simultaneous transmissions is smaller than the number of receive antennas.

3.7.2. Distribution of slots reservations

After receiver j forms the schedule $S(t)$, it reserves a slot for $S(t)$ in the next time frame. Each node maintains a reservation table to record how each slot in a time frame is reserved.

To satisfy the delay constraint of the specific application (D_{max}), the maximum distance between two reserved slots is $D_{rmax} = \left\lfloor \frac{D_{max}}{T_s} \right\rfloor$. On the other hand, the distribution of slots reservations influences the jitter of the channel-access delay. In the ideal case, the reserved slots for each receiver j should be uniformly distributed, the distance between two reserved slots is $D_r = \left\lfloor \frac{LK_s^j}{K_s} \right\rfloor$. However, it may not always be satisfied. Based on the above two considerations, we formulate the problem of reserved slot selection as follows:

$$\begin{aligned} \min \quad & \| t_{j+1} - t_j | - D_r | \quad \forall t_j \in R_t \ \ \forall t_{j+1} \in \overline{R_t} \\ \text{s.t.} \quad & |t_{j+1} - t_j| < D_{rmax}, \end{aligned} \tag{3}$$

where R_t is the set of the previous reserved slots. For each $S(t)$, receiver j tries to reserve a time slot t_{j+1} in the next frame, whose distance between one of the previous reserved slots t_j is closest to the optimal distance D_r. The maximal delay constraint is needed to be satisfied at the same time.

3.7.3. CTS transmission

To avoid the collision of CTS packets from different receivers, each receiver j utilizes the spatial diversity gain to transmit the CTS packet to each selected sender according to the sequence of $S(t)$. The CTS packet includes the channel schedule $S(t)$, and the achieved spatial

multiplexing gain (G_{sm}) for $S(t)$. We first define the *collision-free transmission antenna weight condition* as follows:

$$\begin{aligned} &W_i^H H_{i,j} W_j = 1, \\ &W_i^H H_{i,n} W_n < \varepsilon, \quad n \neq j, \ 0 < \varepsilon \ll 1, \end{aligned} \tag{4}$$

where W_i is the transmission antenna weight of sender i, W_j is the receive antenna weight of receiver j. The number of active receivers in the transmission range of sender i is n, and ε is a small value that satisfies:

$$\mathrm{SINR}_n = \frac{\varepsilon P_i L_i}{\sum_{k \neq i} P_k L_k + \sigma_r^2} < \mathrm{SINR}_{threshold}. \tag{5}$$

In the above equation, σ_r^2 is the background or thermal noise power at the front end of the receiver n; P_i is the transmission power and L_i is the corresponding path-loss factor of i; $\mathrm{SINR}_{threshold}$ is the minimum value of signal to interference plus noise ratio (SINR) that is needed to correctly decode the transmission signal. The *collision-free transmission antenna weight condition* guarantees that, after the transmission antenna weight adjustment of the sender, only the targeted receiver can receive the packet and the other active transmissions are not corrupted.

In ORCHESTRA, a receiver j obtains the antenna weight (W_i) used by the sender i to receive the CTS packet, which is stated in the RTS sent by the sender. Hence, the receiver calculates the antenna weight (W_j) used to transmit the CTS packet according to the *collision-free transmission antenna weight condition*. Compared with the approaches used in NULLHOC and SPACE-MAC, our transmission method for adjusting antenna weights of the CTS packets has two differences:

- We do not require that $W_i^H H_{i,n} W_n = 0$.
- Because W_j is an $M \times 1$ vector initialized randomly by the sender i, the probability that two senders have similar antenna weights for the CTS packet reception is very small.

The above two points guarantees that, even when the channel matrices are highly correlated for different senders ($H_{i,j} \approx H_{i,n}$), we can still find a feasible solution for Eq. (4), thus reducing the possible collisions of CTS transmissions.

Because the number of simultaneous transmissions in the two-hop range is at most twice the number of receive antennas (M), at most $2M$ CTS packets should be sent. The length of the CTS section is $2M \times T_{CTS}$, where T_{CTS} is the transmission time for a CTS packet.

3.8. Conflict resolution

Upon receiving CTS packets from different receivers, nodes compare the G_{sm} and follow the scheduling results with the largest G_{sm}. When the G_{sm} of two CTSs are the same, then the links that are in conflict are not used.

3.9. Scheduled access period

In the scheduled access period, the senders that successfully receive the CTS packets transmit simultaneously using a single antenna. The length of schedule-based access period (T_{data}) is the remaining part of the time slot:

$$T_{data} = T_s - T_{RTR} - M \times T_{PS} - R \times (T_{RTS} + T_{PS}) - 2M \times T_{CTS}. \tag{6}$$

The schedule-based access period is made up of multiple data slots. The length of a data slot ($T_{payload}$) is the time needed to send a data packet with maximum payload length. The number of the data slots (N_{data}) is:

$$N_{data} = \left\lfloor \frac{T_{data}}{T_{payload}} \right\rfloor. \tag{7}$$

3.10. Channel-access example

We use two examples to illustrate the channel-access procedure, as shown in Figs. 4 and 6. In those two examples, we assume that each node has two receive antennas. The upper parts of Figs. 4 and 6 explain how nodes choose time slots across time frames, while the lower parts explain what happens in each time slot.

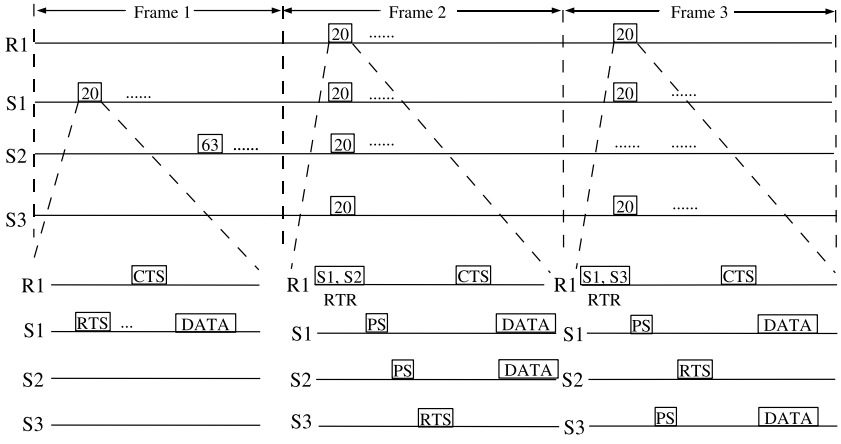

Fig. 4. Channel-access example: single receiver.

3.11. Single receiver

In Fig. 4, we assume that nodes $S1$, $S2$ and $S3$ have packets to send to $R1$, which has two receive antennas.

Note that the RTR section is empty in all the slots of the first time frame. This is because no schedule has been established between the senders and $R1$. In order to illustrate the effects of nodes joining the network, we assume only two nodes ($S1$ and $S2$) have packets to send at the beginning, and $S3$ does not have packets for $R1$ until the second frame. In the first time frame, $S1$ and $S2$ randomly select a slot to transmit their RTS packets. After receiving the confirmation from $R1$, $S1$ and $S2$ transmit in the schedule-based access period. The channel-access procedure of the first time frame is similar to the 802.11 DCF. In the second frame, $R1$ reserves time slot 20 and sends its RTR packet, which indicates that $S1$ and $S2$ have successfully reserved the transmissions. Then $S1$ and $S2$ just need to transmit the pilot symbols in the RTS section and transmit simultaneously in the schedule-based access period of slot 20. $S3$ randomly picks up a mini-slot in the RTS section to transmit its RTS packet, but cannot receive the confirmation from $R1$ during the same time slot. In the third time frame, based on the fair transmission schedule by $R1$, $S3$ should be selected, and we assume $S1$ is also selected. The channel-access procedure is similar to what happens in the second time frame, except that $S2$ sends the RTS packet this time. This procedure continues and each sender is scheduled twice every three time frames.

3.12. Multiple receivers

The network topology is shown in Fig. 5, where $S1$, $S2$ and $S3$ have packets to send to $R1$, while $S4$ and $S5$ have packets to send to $R2$.

The detailed channel-access procedure is shown in Fig. 6.

In the first time frame, $S1$, $S3$ and $S4$ all select time slot 6 to send RTS packets and experience collisions. Accordingly, they back-off and transmit RTSs in other time slots and frames. $S2$ and $S5$ select time slot 27 and 38, respectively. After receiving the CTS from the intended receiver, $S2$ and $S5$ transmit in the schedule-based access period. During the second time frame, $R1$ occupies time slot 27 and sends an RTR packet indicating $S2$ is already reserved. $S2$ transmits pilot symbols, while $S1$ and $S3$ transmits RTS packets, respectively. $R1$ confirms the transmission of $S1$ and $S2$ (or $S3$) through the CTS. In the third time frame, $R1$ indicates that two senders have already reserved transmissions (assume they are $S1$, $S3$), then $S1$ and $S3$ transmit pilot symbols while $S2$ transmit the RTS packet. A similar procedure take place during time slot 38 of time frame 2 and 3, which we omit due to space limitations.

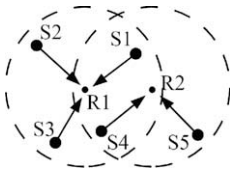

Fig. 5. Multiple receivers topology.

4. Performance analysis

4.1. Frame length

Frame length is an important performance parameter for schedule-based MAC protocol, because it directly influences channel-access delay and spatial reuse in the network.

Lemma 4.1. *The worst-case minimum frame length needed for each node to unicast successfully in one slot every frame in*

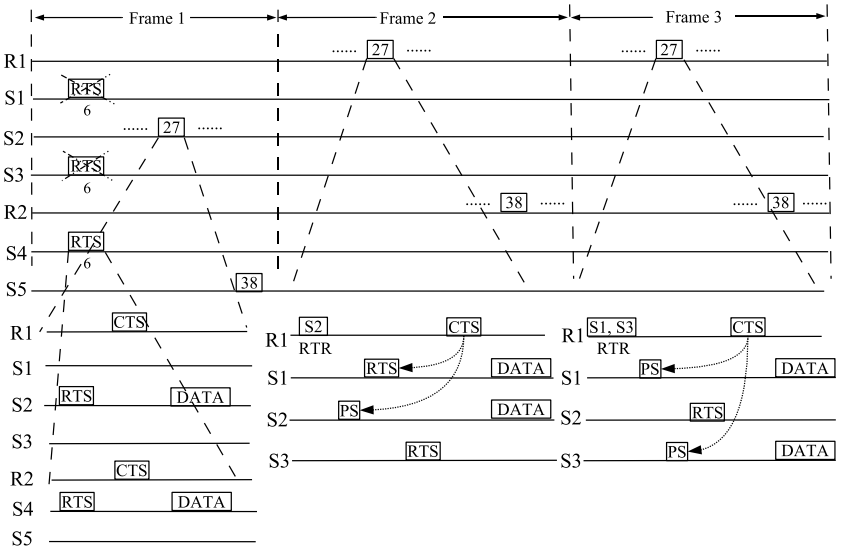

Fig. 6. Channel-access example: multiple receivers.

ORCHESTRA is $\left\lceil \frac{\text{Min}\{d^2+1,N\}}{M} \right\rceil$*, where d is the maximum node degree (number of neighbors a node has) of the network, N is the number of nodes in the network, M is the number of receive antennas.*

Proof. The maximal number of nodes in a two-hop neighborhood is $\text{Min}\{d^2 + 1, N\}$. Because we utilize spatial multiplexing gain in the scheduling-based access period, which allows up to M links to transmit simultaneously, the worst-case minimum frame length needed for each node to unicast successfully in one slot every frame is $\left\lceil \frac{\text{Min}\{d^2+1,N\}}{M} \right\rceil$. □

Lemma 4.2. *The worst-case minimum frame length for each node to unicast successfully to each of its neighbors once every frame in ORCHESTRA is* $\left\lceil \frac{\text{Min}\{2(d^2-d+1),N\}}{M} \right\rceil$ *slots, where d is the maximum node degree (number of neighbors a node has) of the network, N is the number of nodes in the network, M is the number of receive antennas.*

Proof. Let us consider arbitrary transmissions in the two-hop range of node i and node j. There are at most $2(d-1)$ transmissions targeted to node i and j not including the transmissions between i and j. In addition, there are at most $2(d-1)^2$ transmissions from the neighbors of i and j that interfere with the transmissions between i and j. Hence, there are at most $2(d^2 - d + 1)$ transmissions in the two-hop range of i and node j. In the worst case, ORCHESTRA can find a collision-free slot for the intended transmission in up to $\left\lceil \frac{\text{Min}\{2(d^2-d+1),N\}}{M} \right\rceil$ slots. □

If we consider a fixed TDMA protocol using virtual MIMO, the worst-case minimum frame length needed for each node to unicast successfully in one slot every frame is $\lceil \frac{N}{M} \rceil$. TDMA also needs at least $\lceil \frac{N}{M} \rceil$ slots for each node to unicast successfully to each of its neighbors once. Based on Lemma 4.1 and Lemma 4.2 ($N \gg d^2$), ORCHESTRA has a much shorter frame size compared with fixed TDMA.

4.2. Approximate throughput analysis

We assume that new or retransmitted requests to establish reservations arrive at each node according to a Poisson process with an average arrival rate of λ requests per slot. To simplify the analysis, we consider a fully-connected network topology with N nodes. All links are bi-directional or symmetrical. Given that ORCHESTRA increases the spatial reuse of the system through the distributed link scheduling in a two-hop range, a fully-connected network is the worst-case scenario in terms of interference, contention or spatial reuse. Therefore, the throughput of ORCHESTRA for a fully-connected network with N nodes is a lower bound of the throughput of ORCHESTRA for a general topology, where the number of nodes in a two-hop neighborhood is N. The channels are assumed to be error free and have no capture effects. More than M packets overlapped on the same channel at a receiver leads to a collision and no packets involved in it can be received correctly by the receiver. We assume that the reservation information is only updated at the end of each frame. In other words, the number of contention nodes does not change during the frame, this assumption also applies to Section 4.4.

Each node has exactly one buffer that can store only one message. The frame length (L) equals to $\lceil \frac{N}{M} \rceil$ slots and each node intends to reserve one slot per frame. The destination of any data packet from each node is assumed to be uniformly distributed among all its neighbors. All the nodes are synchronized and all channels are slotted with the slot size equal to T_s. Therefore, the total traffic load normalized to slot size is denoted by

$$G = N\lambda T_s.$$

We consider variable-length flows and assume that, on the average, it takes δ slots to send all the data packets in a flow, i.e., the average flow length (AFL) is δ slots. We also assume that the flow length is geometrically distributed, which implies that the probability that a flow ends at the end of a time slot is $q = 1/\delta$.

The system can be fully described by one state variable k ($0 \leqslant k \leqslant N$), which denotes the number of successfully reserved transmissions in a frame. We model the operation of the system as a discrete-time Markov chain, where each state of the Markov chain can transit to any state. A transition may occur when any sender ends its flow or any idle node successfully reserves a transmission slot. Let π_k denote the stationary probability that the system is in state k.

For simplicity, we do not consider the effects of proportional fair scheduling. Because the CTS transmissions are collision-free by means of the spatial diversity gain, and given that there are no hidden terminals in a one-hop range (which excludes the conflict scheduling result resolution), the probability of the number of successful reservations is only dependent on the number of successful RTS transmissions and the traffic pattern. Given that an idle node contends for a slot with probability $p_a = 1 - e^{-\lambda T_s}$, the probability that with i idle nodes there is a successful reservation in an unreserved slot is given by

$$\theta(i) = \binom{i}{1}\left\{ p_a(1-p_a)^{i-1} + \frac{p_a}{R}\sum_{j=1}^{i-1}\binom{i-1}{j}(1-p_a)^j p_a^{i-1-j} \times \left(1-\frac{1}{R}\right)^{i-1-j}\right\}. \tag{8}$$

The first part of Eq. (8) represents the probability that there is just one node that has traffic arrival, the second part represents the probability that some nodes also have traffic arrivals, while choosing different mini-slots of the RTS section to send the RTS packets.

The probability that there are s successful reservations among i idle nodes in t unreserved slots can be expressed recursively as

$$\Theta(i,t,s) = [1-\theta(i)]\Theta(i,t-1,s) + \theta(i)\Theta(i-1,t-1,s-1). \tag{9}$$

The ending conditions are:

$$\Theta(i,t,s) = \begin{cases} [1-\theta(i)]^t, & s = 0, \\ 0, & t < s. \end{cases}$$

For a system that is in state k, we denote the probability that n senders end their flows during a frame as D_k^n,

$$D_k^n = \binom{k}{n} q^n (1-q)^{k-n}, \quad 0 \leqslant n \leqslant k. \tag{10}$$

We condition on the number of senders ending their flows in a frame (n) to calculate the transition probabilities. For the transition from state k in frame f to state l in frame $f+1$, at least $\hat{n} = \max(0, k-l)$ nodes will end their flows in frame f. Therefore, $\hat{n} \leqslant n \leqslant k$, and $s = l-(k-n)$ nodes will successfully reserve a slot in frame $f+1$. The transition probability from state k to state l is

$$P_{lk} = \sum_{n=\hat{n}}^{k} D_k^n \Theta(N-k+n, L-k+n, l-k+n). \tag{11}$$

By solving the global balance equations $\pi_l = \sum_{k=0}^{L} \pi_k P_{lk}$ with the condition $\sum_{l=0}^{L} \pi_l = 1$, we can obtain the average number of successfully reserved slots $\sum_{k=1}^{L} \pi_k k$.

The approximate throughput of ORCHESTRA is defined as the proportion of successfully reserved slots over the whole time frame, that is,

$$S = \frac{\sum_{k=1}^{L} \pi_k k}{L}. \tag{12}$$

As an example, we use $N = 10$ and $R = 5$. Fig. 7 shows the throughput comparison of ORCHESTRA under different traffic loads and different flow lengths. ORCHESTRA can achieve a good system throughput even under high traffic loads.

4.3. Worst-case channel-access delay

At the stationary state, each node should reserve one slot in every time frame. The worst channel-access delay is decided by the following case, node i reserves the first slot of the current frame and the last slot of the next frame:

$$d_{max} = 2L - 2. \tag{13}$$

4.4. Convergence time

To evaluate how quickly ORCHESTRA can reserve the desired number of slots when network topology changes, we analyze the convergence time of ORCHESTRA (we denote the network converges when each node successfully reserves one slot in every frame).

We use the same assumptions used in Section 4.2 and denote the convergence time of node i as T_c. The probability for T_c ending in frame 0 is:

$$P_{T_c}(t) = (1-\theta(N))^{t-1}\theta(N), \quad 1 \leqslant t \leqslant L. \tag{14}$$

In order to compute the probability that T_c ending in frame k ($k > 0$), we need to calculate the expected number of unreserved nodes in frame k (m_k). Given that there are m_k unreserved nodes in frame k, the number of remaining unreserved nodes in frame $k+1$ is:

$$m_{k+1} = m_k - \sum_{i=0}^{m_k} \Theta(m_k, L-i, i)i, \quad k \geqslant 1. \tag{15}$$

Now we can iteratively compute the probability for T_c for a given value t ($P_{T_c}(t)$):

$$P_{T_c}(t) = \left[1 - \sum_{i=1}^{t-1} P_{T_c}(i)\right] \times (1-\theta(m_k))^{t-1}\theta(m_k), \quad kL \leqslant t \leqslant (k+1)L-1, \ m_k \geqslant 1. \tag{16}$$

The average convergence time is then:

$$\overline{T_c} = \sum_{t=1} P_{T_c}(t)t. \tag{17}$$

Fig. 8 shows an example of the average convergence time of ORCHESTRA under different traffic loads. In this example, we vary the traffic arrival rate and take $N = 10$ and $N = 20$. We find that ORCHESTRA converges in up to three time frames. We note that, because m_k (obtained from Eq. (15)) is not necessarily an integer, but Eq. (16) requires an integer input for $\theta(m_k)$, the average convergence time obtained in Fig. 8 is subject to rounding errors. However, we do not care about the exact value of the convergence time, we are mainly interested on its upper bound.

4.5. Protocol overhead

As Figs. 9–11 show, the length of an RTR packet is $16 + 4M$ bytes (we note that there are up to M successful

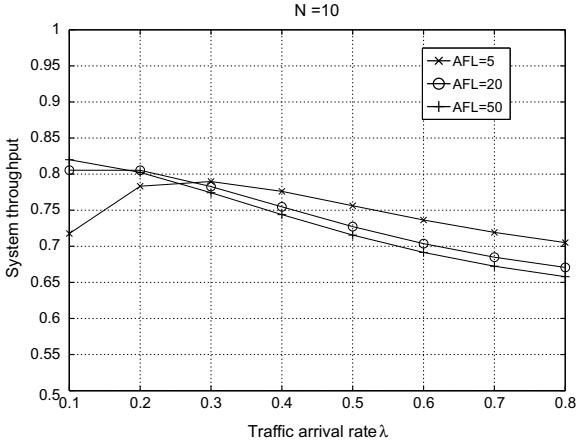

Fig. 7. Throughput comparisons under different traffic load.

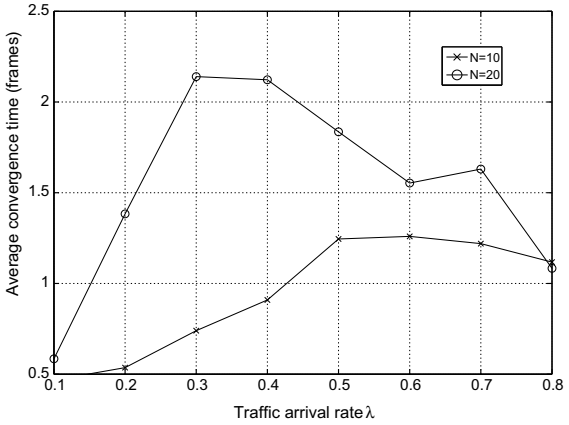

Fig. 8. Average convergence time under different traffic loads.

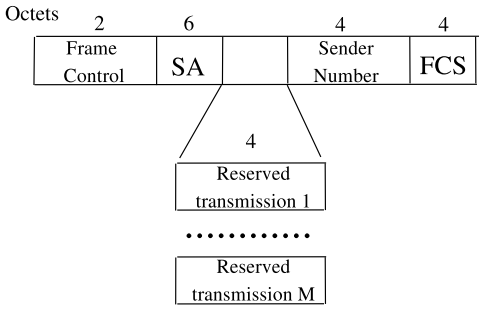

Fig. 9. RTR packet format.

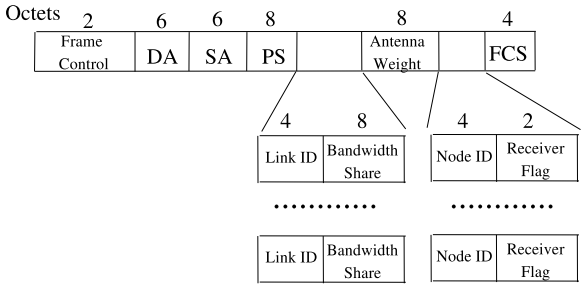

Fig. 10. RTS packet format.

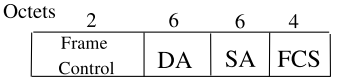

Fig. 11. CTS packet format.

transmission reservations). The length of an RTS packet is $34 + 12K_s^1 + 6N_s^1$ bytes, where K_s^1 is the number of transmissions in the on-hop range and N_s^1 the number of one-hop neighbors. The length of CTS packet is 18 bytes.

We assume the data rate is 54 Mbps, the length of pilot symbols is 8 bytes. We take K_s^1 as 20, N_s^1 equals to 40 and R equals to 5 for example, then the protocol overhead ratio is 32.9%.

5. Performance comparison

We compare the performance of ORCHESTRA with two alternative designs: DCF-MIMO and NAMA-MIMO.

In DCF-MIMO, an RTS/CTS handshake is used to eliminate the hidden terminal effect and pilot symbols are sent in the RTS packet to the receiver. The RTS/CTS packets are sent with a low transmission rate (R_{basic}), while the DATA/ACK packets are sent with a high transmission rate (R_{data}), which utilizes the spatial multiplexing gain of MIMO links. DCF-MIMO is the most direct extension of IEEE 802.11 DCF for a MIMO system.

NAMA-MIMO extends the NAMA scheme [12]. NAMA uses a hash function that takes the node identifier and the current time slot number as inputs to derive a random priority for every neighbor within two hops. If a node has the highest priority, it can access the channel within the corresponding time slot. The advantage of NAMA is that it incurs very small communication overhead in building the dynamic channel-access schedule. NAMA-MIMO extends NAMA by using the spatial multiplexing gain in the payload transmission of each slot.

5.1. Physical layer transmission rate comparison

To make a fair comparison between the MIMO and the virtual MIMO system, we need to derive an approximate physical layer rate. The physical layer transmission rate is:

$$Rate = \mathrm{C} \times \mathrm{BW}, \tag{18}$$

where C is the channel capacity and BW is the channel bandwidth. We assume that the MIMO and the virtual MIMO systems have the same total bandwidth and unit variance noise. There is no spatial interference and both systems can achieve their channel capacity upper bounds. Hence, we can obtain the following approximate relationship of the total transmission rate of virtual MIMO (R_{vmimo}) and MIMO (R_{mimo}) system from Eqs. (1) and (18):

$$\frac{R_{\text{vmimo}}}{R_{\text{mimo}}} \approx \frac{\log(1+P)}{\log(1+P/M)}. \tag{19}$$

Based on the default transmission power and data rate settings in the Qualnet simulator [13], which are indicated in Table 1, we obtain the transmission rate comparison of MIMO and virtual MIMO systems with different number of antennas shown in Fig. 12. These results demonstrate that a MIMO system always achieves a lower total transmission rate than a virtual MIMO system. The ratio of R_{vmimo} over R_{mimo} increases with the number of antennas but decreases with the additional transmission power.

Table 1
Tx power and Tx data rate relationship.

Tx power (dB m)	Tx data rate (Mbps)
20.0	6,9
19.0	12,18
18.0	24,36
16.0	48,54

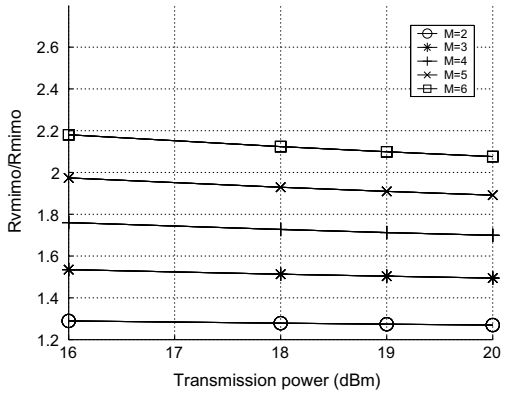

Fig. 12. Tx rate comparison of MIMO and virtual MIMO.

Table 2
Tx rate of virtual MIMO system.

Number of antennas (M)	R_{vmimo} (Mbps)	R_{link} (Mbps)
2	69.63	34.82
4	95.04	23.76
6	117.75	19.63

Now we assume that R_{mimo} is fixed at 54 Mbps and vary the number of receive antennas. Then, according to Fig. 12, we can compute the corresponding transmission rate of the virtual MIMO system (R_{vmimo}) and the maximum transmission rate of each link (R_{link}), as Table 2 shows.

5.2. Simulation settings

We assume that each receiver has four receive antennas and uses 802.11a as the physical layer. The MIMO transmission rate is 54 Mbps. The transmission power is 16 dB m. The receive threshold for the 54 Mbps data rate is −63 dB m, the corresponding transmission range is around 40 m. All these simulation parameters are the default settings in Qualnet [13]. According to Table 2, the total transmission rate of the virtual MIMO system is 95.04 Mbps, while the maximum transmission rate for each link is 23.76 Mbps. The duration of the simulation is 100 s. A time frame consists of 100 time slots ($L = 100$). The simulations are repeated with 10 different seeds to average the results for each scenario. We set the path-loss factor as $\alpha = 4$, the number of mini-slots in the RTS section (R) is 5, and the delay constraint (D_{max}) is 20 ms.

5.3. Multiple-sender single-receiver topology

We generate a static topology with 20 nodes acting as receivers and randomly distributed across a $300 \times 300\ m^2$ area. As Fig. 13 shows, in the transmission range of each receiver, there are n senders, where n is a random number uniformly distributed in $[1, N_s]$. We set up a constant bit rate (CBR) flow for each sender–receiver pair and vary the inter-packet time to evaluate the performance. The packet length of the CBR flow is 512 bytes.

We made two groups of comparisons. First, we set N_s to 6, and compare the performance of DCF-MIMO and NAMA-MIMO with the performance of ORCHESTRA. Second, we compare the performance of ORCHESTRA under three different values of N_s ($N_s = 6, 12, 18$). For the cases in which $N_s = 12$ and $N_s = 18$, because the average number of senders (6 and 9) is higher than the number of receive antennas (4), these scenarios illustrate the system capacity of the virtual MIMO system.

Fig. 14 shows the average throughput at each receiver. Comparing DCF-MIMO and NAMA-MIMO with ORCHESTRA when $N_s = 6$, we find that the system throughput increases significantly when virtual MIMO is used. With the increase of N_s, we add more traffic flows into the network and the system becomes saturated when $N_s = 12, 18$. The increase of the number of traffic flows introduces more contentions and the average throughput of each flow decreases, as Fig. 15 illustrates. In Fig. 16, we compare the average channel-access delay of ORCHESTRA with that of DCF-MIMO and NAMA-MIMO. We find that ORCHESTRA provides a bounded channel-access delay which is much smaller than in the other two schemes. This is because ORCHESTRA finds transmission opportunities for each packet that satisfy the delay constraints by means

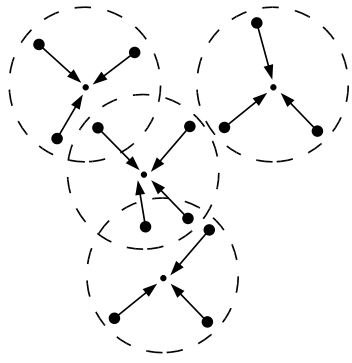

Fig. 13. Multiple-sender single-receiver topology.

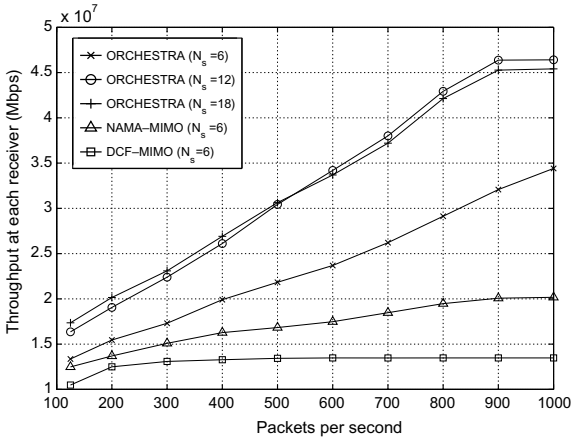

Fig. 14. Throughput.

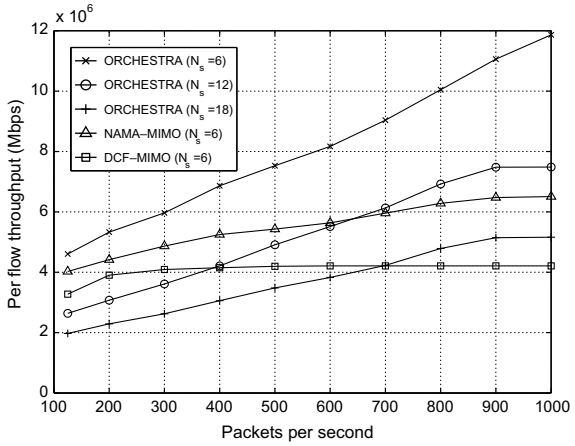

Fig. 15. Per flow throughput.

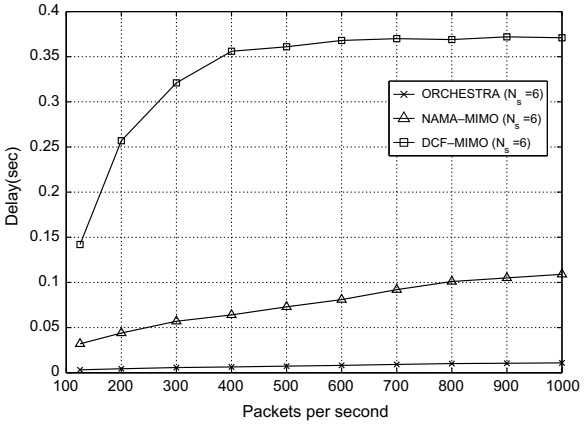

Fig. 16. Delay ($N_s = 6$).

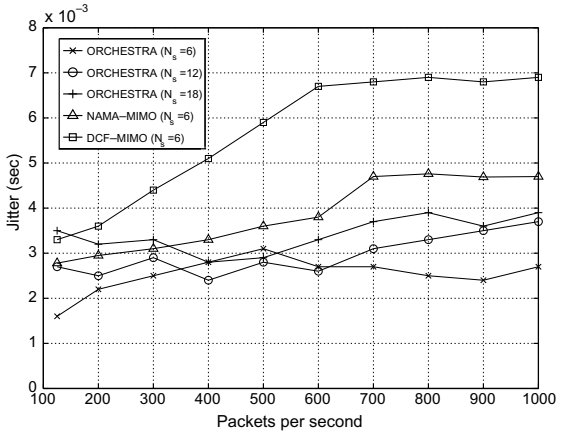

Fig. 18. Jitter.

of reservation. If the channel-access delay of a packet exceeds the delay constraint, ORCHESTRA cannot find a feasible schedule for this packet through Eq. (3), and it is discarded silently. By contrast, in DCF-MIMO and NAMA-MIMO, packets are continuously transmitted over the channel if they do not exceed the retransmission limits. This approach wastes the scarce wireless channel bandwidth and degrades the delay of real-time applications. The delay comparison of ORCHESTRA with different values of N_s is shown in Fig. 17. From Fig. 18, we can observe that ORCHESTRA smoothes the delay jitter by the approximating a uniform distribution of transmission opportunities. To illustrate the effect of proportional fair scheduling, we use the flows targeted for a specific receiver, and the per flow throughput comparison is shown in Fig. 19. It is apparent that ORCHESTRA achieves good fairness across different traffic flows. ORCHESTRA outperforms NAMA-MIMO because of three reasons. First, in NAMA-MIMO, a node may probabilistically derive a low priority for a long period of time and never get access to the channel. Second, there may be chain effects to the channel-access opportunities in which the priorities of nodes cascade from high priority to low priority across the network. This in turn reduces the spatial reuse of the system. Third, channel bandwidth may also be wasted when a node does not have data to send in the allocated time slot. The waste of bandwidth causes the starvation of some of the nodes, NAMA interacts

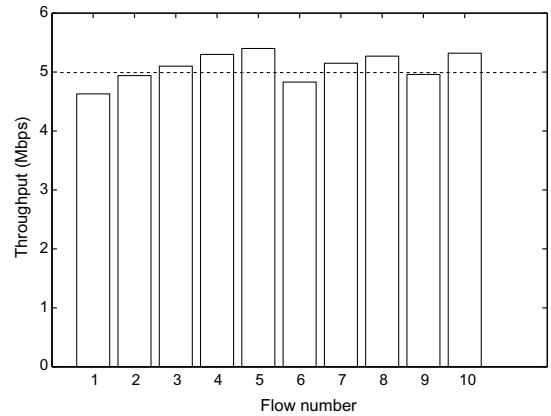

Fig. 19. Per flow throughput at single receiver.

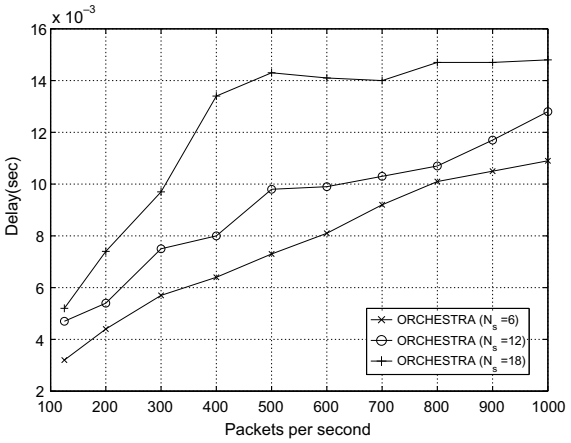

Fig. 17. Delay of ORCHESTRA ($N_s = 6, 12, 18$).

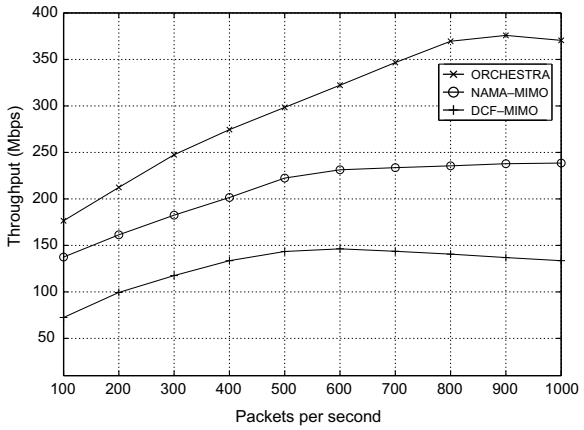

Fig. 20. Average system throughput for random topology.

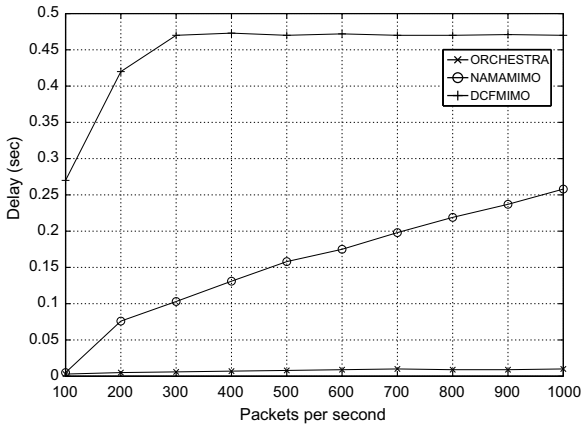

Fig. 21. Average delay for random topology.

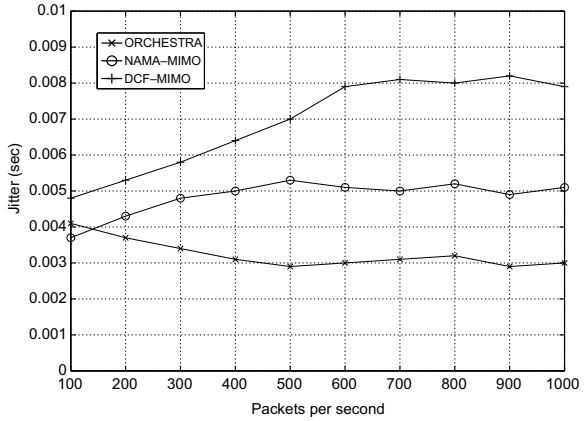

Fig. 22. Average jitter for random topology.

badly with certain applications that are sensitive to the delay, such as TCP congestion control [14], AODV route update mechanisms [15], or voice over wireless IP.

5.4. Random topology

We generate 10 topologies with 50 nodes uniformly distributed across a $500 \times 500\ m^2$ area. We set up 20 CBR flows between randomly selected sender–receiver pairs, such that senders and receivers are always more than two hops away from each other. The packet length of the CBR flows is 1024 bytes. The simulation results are shown in Figs. 20–22. The results illustrate that, even in random topology, ORCHESTRA can still increase the system throughput at least two times, while attaining a bounded channel-access delay at the same time.

6. Discussion

ORCHESTRA adapts a schedule-based MAC to the use of MIMO radios instead of a contention-based MAC. The key reason for this choice is the ability to sustain high throughput under high traffic loads, while providing Quality-of-Service (QoS) support for real-time applications. We assume that clock synchronization among all the stations in the network is achieved through GPS or other multi-hop time synchronization schemes [16,17]. The accuracy of time synchronization will partially influence the performance of ORCHESTRA, and the guarding time between the time slots will also increase the protocol overheads. How to achieve global synchronization in wireless ad hoc networks will impact the feasibility of ORCHESTRA. We did not discuss such problems due to the page limits. More detailed discussions on time synchronization can be found in [18,17].

7. Conclusion

We proposed a joint PHY/MAC optimization approach based on spatial diversity gain to reduce the collisions of control packets, while utilizing the spatial multiplexing gain to increase the transmission rates of data packets. The advantage of ORCHESTRA is that enjoys the high throughput merit of probabilistic channel-access schemes, the bounded access delay characteristics of reservation-based schemes, and the multiplexing gains attainable with virtual MIMO.

ORCHESTRA is suitable for ad hoc networks in which voice and data services must be provided, and takes advantage of multiple antennas much more efficiently than simply applying MIMO techniques at the physical layer to conventional contention-based or dynamic-scheduling channel-access schemes.

References

[1] L. Zheng, D. Tse, Diversity and multiplexing: a fundamental tradeoff in multiple-antenna channels, IEEE Transactions on Information Theory 49 (5) (2003) 1073–1096.
[2] G. Foschini, G. Golden, R. Valenzuela, P. Wolniansky, Simplified processing for high spectral efficiency wireless communication employing multi-element arrays, IEEE Journal of Selected Areas in Communications 17 (1999) 1841–1852.
[3] J. Anderson, Antenna arrays in mobile communications: gain, diversity, and channel capacity, IEEE Antennas and Propagation Magazine 42 (2000) 12–16.
[4] K. Sundaresan, R. Sivakumar, M.A. Ingram, T.-Y. Chang, A fair medium access control protocol for ad-hoc networks with MIMO links, in: Proceedings of IEEE INFOCOM, March 2004, pp. 2559–2570.
[5] M. Hu, J. Zhang, MIMO ad hoc networks: medium access control, satuation throughput, and optimal hop distance, Journal of Communications and Networks (2004) (Special Issue on Mobile Ad Hoc Networks).
[6] J.C.Mundarath, P. Ramanathan, B. Veen, NULLHOC: a MAC protocol for adaptive antenna array based wireless ad hoc networks in multipath environments, in: Proceeding of IEEE Global Telecommunications Conference, vol. 5, 2004, pp. 2765–2769.
[7] J.-S. Park, A. Nandan, M. Gerla, H. Lee, SPACE-MAC: enabling spatial resuse using MIMO channel-aware MAC, in: Proceeding of IEEE International Conference on Communications, 2005.
[8] M. Dohler, Virtual Antenna Arrays, Kings College London, Ph.D. Thesis, 2003.
[9] G. Jakllari, S. Krishnamurthy, M. Faloutsos, P. Krishnamurthy, O. Ercetin, A framework for distributed spatio-temporal communications in mobile ad hoc networks, in: Proceedings of IEEE INFOCOM, 2006.
[10] G.J. Foschini, M.J. Gans, On limits of wireless communications in a fading environment when using multiple antennas, Wireless Personal Communications 6 (1998) 311–355.
[11] E. Telatar, Capacity of multi-antenna Gaussian channels, European Transactions on Telecommunications 10 (6) (1999) 585–595.

[12] L. Bao, J.J. Garcia-Luna-Aceves, A new approach to channel access scheduling for ad hoc networks, in: ACM Seventh Annual International Conference on Mobile Computing and Networking (Mobicom), 2001.
[13] Qualnet Simulator, Scalable Network Technologies. <http://www.scalable-networks.com/>.
[14] T. Socolofsky, C. Kale, RFC 1180 – A TCP/IP Tutorial, January 1991.
[15] C. Perkins, E. Belding-Royer, S. Das, RFC 3561– Ad hoc On-Demand Distance Vector (AODV) Routing, July 2003.
[16] J.P. Sheu, C.M. Chao, C.W. Sun, A clock synchronization algorithm for multi-hop wireless ad hoc networks, in: Proceedings of IEEE ICDCS, 2004, pp. 574–581.
[17] K. Römer, E. Zurich, Time synchronization in ad hoc networks, in: Proceedings of ACM Mobihoc, 2001.
[18] Carlos H. Rentel, Network Time Synchronization and Code-based Scheduling for Wireless Ad Hoc Networks, Ph.D. Thesis, Carleton University, Ontario, Canada, January 2006.

Xin Wang received the B.S. and M.S. degrees in electronic engineering from Tsinghua University, Beijing, China, in 2002 and 2005, respectively. Since 2005, he has been a Ph.D. student of the computer communication research group (CCRG) in Department of Computer Engineering, University of California, Santa Cruz, US. His research interests include performance evaluation and protocol design, cross layer optimization in wireless networks. He is a student member of IEEE and ACM.

J.J. Garcia-Luna-Aceves holds the Jack Baskin Chair of Computer Engineering at the University of California, Santa Cruz (UCSC), and is a Principal Scientist at the Palo Alto Research Center (PARC). Prior to joining UCSC in 1993, he was a Center Director at SRI International (SRI) in Menlo Park, California. He has been a Visiting Professor at Sun Laboratories and a Principal of Protocol Design at Nokia. He has published a book, more than 300 papers, and 17 US patents. He has directed 25 Ph.D. theses and 20 M.S. theses since he joined UCSC in 1993.

He has published a book, more than 330 papers, and 24 US patents. He has directed 25 Ph.D. theses and 20 M.S. theses since he joined UCSC in 1993. He is the General Chair of the ACM Mobicom 2008 conference. He has been the General Chair of the IEEE SECON 2005 Conference; Program Co-Chair of ACM MobiHoc 2002 and ACM Mobicom 2000; Chair of the ACM SIG Multimedia; General Chair of ACM Multimediaí93 and ACM SIGCOMMí88; and Program Chair of IEEE MULTIMEDIA í92, ACM SIGCOMMí87, and ACM SIGCOMMí86. He has served in the IEEE Internet Technology Award Committee, the IEEE Richard W. Hamming Medal Committee, and the National Research Council Panel on Digitization and Communications Science of the Army Research Laboratory Technical Assessment Board. He has been on the editorial boards of the IEEE/ACM Transactions on Networking, the Multimedia Systems Journal, and the Journal of High Speed Networks. He is a Fellow of the IEEE and is listed in Marquis Whoís Who in America and Whoís Who in The World. He is the co-recipient of Best Paper Awards at SPECTS 2007, IFIP Networking 2007, and IEEE MASS 2005 conferences, and the Best Student Paper Award of the 1998 IEEE International Conference on Systems, Man, and Cybernetics. He received the SRI International Exceptional-Achievement Award in 1985 for his work on multimedia communication and in 1989 for his work on routing algorithms.

Hamid R. Sadjadpour received his B.S. and M.S. degrees from Sharif University of Technology with high honor and Ph.D. degree from University of Southern California in 1986, 1988 and 1996, respectively. After graduation, he joined AT&T as a member of technical staff, later senior technical staff member and, finally, Principal member of technical staff at AT&T Lab. in Florham Park, NJ until 2001. In fall 2001, he joined University of California, Santa Cruz (UCSC) where he is now an Associate Professor.

He has served as technical program committee member in numerous conferences and as chair of communication theory symposium at WirelessCom 2005, and chair of communication and information theory symposium at IWCMC 2006, 2007 and 2008 conferences. He has been also Guest editor of EURASIP on special issue on Multicarrier Communications and Signal Processing in 2003 and special issue on Mobile Ad Hoc Networks in 2006, and is currently Associate editor for Journal of Communications and Networks (JCN). He has published more than 90 publications. His research interests include space–time signal processing, scaling laws for wireless ad hoc networks, performance analysis of ad hoc and sensor networks, and MAC layer protocols for MANETs. He is the co-recipient of International Symposium on Performance Evaluation of Computer and Telecommunication Systems (SPECTS) 2007 best paper award. He holds more than 13 patents, one of them accepted in spectrum management of T1.E1.4 standard.